Energy 160 (2018) 257–274

Contents lists available at ScienceDirect

Energy

journal homepage: www.elsevier.com/locate/energy

A novel stochastic energy management of a microgrid with various types of distributed energy resources in presence of demand response programs

Alireza SoltaniNejad Farsangi, Shahrzad Hadayeghparast, Mehdi Mehdinejad, Heidarali Shayanfar*

Center of Excellence for Power Systems Automation and Operation, School of Electrical Engineering, Iran University of Science and Technology, Tehran, Iran

ARTICLE INFO

Article history:
Received 25 January 2018
Received in revised form
24 May 2018
Accepted 20 June 2018
Available online 26 June 2018

Keywords:
Microgrid energy management
Distributed energy resource (DER)
Demand response programs (DRPs)
Uncertainty
Two-stage stochastic programming
Plug-in electric vehicles (PEVs)

ABSTRACT

In this paper, the energy management of a microgrid including wind turbine, PhotoVoltaic (PV) modules, Combined Heat and Power (CHP) systems, fuel cells, power only units, heat only unit, Plug-in Electric Vehicles (PEVs), and thermal energy storage resources for supplying electrical and thermal loads is presented. For achieving a better management on demand side, both price-based and incentive-based Demand Response Programs (DRPs) have been used and their impacts on reducing the operational cost of microgrid in both grid-connected and island modes have been investigated. Also, the uncertainty of price, load, wind speed and solar radiation are taken into account in order to obtain more realistic results. By discretization of Probability Distribution Function (PDF) of each uncertain parameter, a set of scenarios is generated. Then, using a scenario reduction method based on mixed-integer linear optimization, the set of reduced scenarios is obtained. Two-stage stochastic programming approach is used to minimize the operational cost in microgrid energy management. The proposed method for microgrid energy management has been evaluated in three modes: grid-connected, grid-connected with DRPs, and island mode with DRPs.

1. Introduction

With increasing electricity consumption in recent years, some components like generation cost, emission, reliability and quality of electrical energy have gained more importance. Microgrids are structures that can improve all the above-mentioned components in supplying electrical loads. A microgrid consists of Distributed Generations (DGs), energy storages and loads (electrical and thermal) which can operate in grid-connected and island modes. The microgrid normally operates connected to the main grid but when some disturbances such as outage occur in the upstream network, the microgrid disconnects from main grid and goes to the island mode and functions autonomously. As a result, the reliability of the energy supply will be increased. The cost of generation and emission should also be considered in energy generation. Consequently, there is a need for an energy management system that can determine the contribution of each resource in supplying the consumer energy. Studies that are carried out in the field of microgrid energy management can be categorized from various perspectives such as type of DER resources, formulation of the energy management problem, uncertainty, solving method, and various types of consumption management methods. In Table 1, some of the references are categorized according to the above-mentioned perspectives.

In fact, DGs are energy resources with low capacities that are usually connected to distribution networks and also close to the consumers. This proximity of DG to consumer has some benefits such as loss reduction, decreasing transmission costs, increasing quality, and so on. The aforementioned resources are divided into two broad categories, namely renewable and traditional. Furthermore, Energy storage systems can also be used as a microgrid resource and play a significant role in energy management and dynamic issues related to microgrids. The energy storage systems can also be divided into two general categories, thermal and electrical. Studies have used different types of DG resources and storage systems to supply thermal and electrical loads. In Ref. [1],

* Corresponding author.
E-mail addresses: alireza_soltani@elec.iust.ac.ir (A. SoltaniNejad Farsangi), sh_hadayeghparast@vu.iust.ac.ir (S. Hadayeghparast), m.mehdinejad1369@gmail.com (M. Mehdinejad), hashayanfar@gmail.com, hashayanfar@iust.ac.ir (H. Shayanfar).

https://doi.org/10.1016/j.energy.2018.06.136
0360-5442/

Nomenclature

Sets

t	Set of time periods, ranging from 1 to 24
j	Set of fuel cell units, ranging from 1 to N^{fc}
i	Set of CHP units, ranging from 1 to N^{chp}
v	Set of PEVs, ranging from 1 to N^{v}
q	Set of power only units, ranging from 1 to N^{po}
θ	Set of scenarios, ranging from 1 to N^{θ}
ζ	Set of blocks related to operational cost of power only units

Scenario-Dependent Parameters

$sor_{t,\theta}$	Solar radiation at hour t and scenario θ
$T_{C_{t,\theta}}$	Solar cell temperature at hour t and scenario θ (°C)
$V^{w}_{t,\theta}$	Wind speed at hour t and scenario θ (m/s)
$Price^{grid}_{t,\theta}$	Energy market price at hour t and scenario θ ($/kWh)
$P^{load}_{t,\theta}$	Total electrical load at hour t and scenario θ (kW)
$P^{Demand}_{t,\theta}$	Total electrical load after load shifting at hour t and scenario θ (kW)
$P^{wind}_{t,\theta}$	Output power of wind turbine at hour t and scenario θ (kW)
$P^{pv}_{t,\theta}$	Output power of PV modules at hour t and scenario θ (kW)

Input Parameters

CHP

N^{chp}	Number of CHP units
λ^{NG}	Price of natural gas ($/kWh)
η^{chp}	Efficiency of CHP units (%)
$C^{chp,u}_{i}$	Startup cost of CHP unit i ($)
$C^{chp,d}_{i}$	Shutdown cost of CHP unit i ($)
β_{gain}	Excess heat of CHP unit i at shutdown time (kWth h)
β_{loss}	Heats loss of CHP unit i at startup time (kWth h)

Power Only

$P^{MAX}_{q,\zeta}$	Rated power of block ζ related to operational cost of power only unit q (kW)
R^{up}_{q}	Ramp up rate of power only unit q (kW/h)
R^{down}_{q}	Ramp down rate of power only unit q (kW/h)
MUT_q	Minimum Up Time of power only unit q (h)
MDT_q	Minimum Down Time of power only unit q (h)
N^{po}	Number of power only units
N^{b}	Number of blocks related to operational cost of power only unit
$\lambda^{po}_{q,\zeta}$	The price of power of power only unit q at block ζ ($/kWh)

Heat Only

λ^{ho}	The price of power of heat only unit ($/kWth h)
$T^{ho,max}$	Rated power of heat only unit (kWth)

Fuel Cell

$Cap^{fc,h2,min}_{j}$	Minimum hydrogen storage capacity of fuel cell unit j (kg)
$Cap^{fc,h2,max}_{j}$	Maximum hydrogen storage capacity of fuel cell unit j (kg)
$H^{fc,dch,max}_{j}$	Maximum hydrogen discharge rate of fuel cell j (kg/h)
$P^{fc}_{j,max}$	Maximum output power of fuel cell unit j (kW)
$P^{fc}_{j,min}$	Minimum output power of fuel cell unit j (kW)
$\eta^{fc,st}_{j}$	Hydrogen storage efficiency of fuel cell unit j (%)
N^{fc}	Number of fuel cell units
$C^{fc,pump}_{j}$	Hydrogen pumping cost of fuel cell unit j ($/kWh)
$C^{fc,u}_{j}$	Startup cost of fuel cell unit j ($)
$C^{fc,d}_{j}$	Shutdown cost of fuel cell unit j ($)

PV

AT_t	Ambient temperature at hour t (°C)
N_{OT}	Nominal operating temperature of solar cell (°C)
FF	Fill factor of PV module
I_{MPP}	Current at maximum power point of PV module (A)
I_{sc}	Short circuit current of PV module (A)
K_i	Current temperature coefficient of PV module (A/°C)
K_v	Voltage temperature coefficient of PV module (V/°C)

Wind Turbine

V_{ci}	Cut-in speed (m/s)
V_r	Rated speed (m/s)
V_{co}	Cut-out speed (m/s)
p_r	Nominal power of wind-turbine (kW)

Demand Response

B^{up}_{t}	Maximum participation factor for increasing demand in price-based DRP (%)
B^{down}_{t}	Maximum participation factor for decreasing demand in price-based DRP (%)

(*continued*)

$\beta^{I}, \beta^{II}, \beta^{III}$	Price of load readiness at first, second and third level of incentive-based DRP ($/kWh)
$\alpha^{I}, \alpha^{II}, \alpha^{III}$	Maximum participation percentage of electrical loads at first, second and third level of incentive-based DRP (%)
β^{elc}	Price of load curtailment ($/kWh)
β^{ens}	Price of ENS ($/kWh)
PEV	
η_v^c	Charging efficiency of PEV v (%)
η_v^d	Discharging Efficiency of PEV v (%)
E_v^0	Initial level of energy in PEV v (kWh)
SOC_v^{Min}	Minimum state of charge in PEV v (kWh)
SOC_v^{Max}	Maximum state of charge in PEV v (kWh)
Ω_v	Efficiency of The PEV v (kW/km)
Pc_v^{Min}	Minimum charging rate of PEV v (kW/h)
Pc_v^{Max}	Maximum charging rate of PEV v (kW/h)
Pd_v^{Min}	Minimum discharging rate of PEV v (kW/h)
Pd_v^{Max}	Maximum discharging rate of PEV v (kW/h)
Heat Buffer Tank	
B_{min}	Minimum level of energy in heat buffer tank (kWth)
B_{max}	Maximum level of energy in heat buffer tank (kWth)
$T^{b,c,max}$	Maximum charging rate of heat buffer tank (kWth/h)
$T^{b,d,max}$	Maximum discharging rate of heat buffer tank (kWth/h)
$\eta^{b,c}$	Charging efficiency of heat buffer tank (%)
$\eta^{b,d}$	Discharging efficiency of heat buffer tank (%)
Variables	
CHP	
$P_{t,i}^{chp}$	Electrical output power of CHP unit i at time t (kW)
$T_{t,i}^{chp}$	Thermal output power of CHP unit i at time t (kW)
$I_{t,i}^{chp}$	Spinning state of CHP unit i at time t
$SU_{t,i}^{chp}$, $SD_{t,i}^{chp}$	Start-up and shut-down states of CHP unit i at time t
Power Only	
$P_{t,q,\zeta,\theta}^{po}$	Output power of Power only unit q at time t, block ζand scenario θ (kW)
$U_{t,q,\theta}^{po}$	Spinning state of Power only unit q at time t and scenario θ
Heat Only	
T_t^{ho}	Thermal output power of heat only unit at time t (kWth)
Fuel Cell	
$P_{t,j}^{fc,e}$	Electrical output power of fuel cell unit j at time t (kW)
$P_{t,j}^{fc,h}$	Equivalent electrical power of hydrogen generated by fuel cell unit j at time t (kW)
$T_{t,j}^{fc}$	Thermal output power of fuel cell unit j at time t (kWth)
$TER_{t,j}^{fc}$	Thermal to electrical power ratio of fuel cell unit j at time t
$PLR_{t,j}$	Electrical output power to rated power of fuel cell unit j ratio at time t
$\eta_{t,j}^{fc}$	Efficiency of fuel cell unit j at time t
$H_{t,j}^{fc,dch}$	Amount of discharging hydrogen in fuel cell unit j at time t (kg)
$H2_{t,j}^{fc}$	Amount of hydrogen stored in fuel cell unit j at time t (kg)
$I_{t,j}^{fc}$	Commitment state of the fuel cell unit j at time t
$SU_{t,j}^{fc}$, $SD_{t,j}^{fc}$	Start-up and shut-down states of fuel cell unit j at time t
$H_{t,j}^{fc,h}$	The amount of produced hydrogen of fuel cell j at time t (kg)
Demand Response	
$P_{t,\theta}^{Demand}$	Electrical load after the implementation of price-based DRP at time t and scenario θ (kW)
$DR_{t,\theta}^{up}$	Amount of load increased by implementation of price-based DRP at time t and scenario θ (kW)
$DR_{t,\theta}^{down}$	Amount of load decreased by implementation of price-based DRP at time t and scenario θ (kW)
$P_{t,\theta}^{elr,I}$, $P_{t,\theta}^{elr,II}$, $P_{t,\theta}^{elr,III}$	Committed Electrical load at first, second and third level of incentive-based DRP at hour t and scenario θ (kW)
$COST_{t,\theta}^{elr}$	Cost of load readiness at time t and scenario θ ($)
$P_{t,\theta}^{elc}$	Amount of load curtailment at time t and scenario θ (kW)
$COST_{t,\theta}^{elc}$	Cost of load curtailment at time t and scenario θ ($)
$P_{t,\theta}^{ens}$	Amount of ENS at time t and scenario θ (kW)
$COST_{t,\theta}^{ens}$	Cost of ENS at time t and scenario θ (kW)
PEV	
$SOC_{t,v,\theta}$	State of charge of PEV v at time t and scenario θ (kWh)
$Pcv_{t,v,\theta}$	Amount of charging power of PEV v at time t and scenario θ (kW)
$Pdv_{t,v,\theta}$	Amount of discharging power of PEV v at time t and scenario θ (kW)
$Uc_{t,v,\theta}$	Charging state of PEV v at time t and scenario θ
$Ud_{t,v,\theta}$	Discharging state of PEV v at time t and scenario θ
Heat Buffer Tank	

(*continued on next page*)

(*continued*)

B_t	Amount of energy stored in heat buffer tank (kWth h)
$T_t^{b,c}$	Charging power of heat buffer tank (kWth)
$T_t^{b,d}$	Discharging power of heat buffer tank (kWth)
Grid	
$P_{t,\theta}^{eql}$	Served electrical load at time t and scenario θ (kW)
$P_{t,\theta}^{G}$	Exchanged power with grid at time t and scenario θ (kW)

renewable DGs, which include wind turbine and PV, with fuel cells and power only units have been used to supply electrical load, but thermal load has not been considered. Considering the benefits of CHP systems such as reducing emission and increasing energy efficiency, the use of these resources can play a significant role in reducing cost and emission. In Ref. [2], CHP has been applied to generate thermal and electrical power, but the energy storage devices have not been used. The Feasible Operating Region (FOR) of CHP is also considered in Ref. [3], and the power generation cost of CHP is linearly modeled in the total cost function. Added to that, both thermal and electrical energy storage devices are also utilized. In Ref. [4 and 5], in addition to considering FOR of CHP, cost of power generation is modeled as a nonlinear relationship of the electrical and thermal output power of CHP in the cost function.

In the process of implementing the energy management system, a number of input parameters do not have a certain amount and consequently demonstrate a probable behavior. Considering the aforesaid uncertainties can increase the applicability of obtained solutions under real operating conditions. The number of uncertain parameters is different in each reference, depending on the problem statement and the assumptions. A stochastic framework is proposed in Ref. [6] that examines the impact of load, market price, PV and wind turbine generation uncertainties on optimal operational management of microgrids. Initially, using PDF of each uncertain parameter and the roulette wheel mechanism, several scenarios are generated. Then, in the process of scenario reduction, scenarios that are more probable and similar are selected. For modeling the uncertainty existing in the market price, wind speed, and solar radiation, a scenario-based approach has been used in Ref. [2].

Scenario generation and reduction techniques are employed in Ref. [7] to investigate the effect of wind power uncertainty on system operation. Given the fact that the microgrid is connected to upstream network through which power sales and purchase take place, electricity price in the upstream network can also be modeled as an uncertain parameter that references [3] and [6] have taken into account this uncertainty. Many methods of uncertainty modeling attempt to treat the behavior of an uncertain parameter as a set of scenarios.

As the number of uncertain parameters grows, the number of generated scenarios and the time spent on calculations also increases. As a result, scenario reduction technique has gained popularity and since then several methods have been proposed in this regard. A scenario reduction algorithm based on probability distance is proposed in Ref. [8], that attempts to select the closest set of reduced scenarios that have probabilistic behavior close to the initial set. A number of references use an optimization method for the selection process of scenarios. An optimal scenario-reduction algorithm (OSCAR) is presented in Ref. [9] which is formulated as a mixed-integer linear optimization problem. This method not only reduces the probability distance between the set of previous scenarios and the new set, but also decreases the difference between the best and worst possible output from the initial set of scenarios versus the reduced set of scenarios. In deterministic-unlike stochastic-modeling, certainty of data is a basic assumption. Some studies such as [4,5,10–12,16] have used deterministic modeling to formulate the management of microgrid resources.

Demand response is a change in the normal electrical power consumption pattern of consumers. DRPs fall into two broad categories, namely price-based and incentive-based. Therefore, changes in the pattern of electricity consumption are the responses that are given to changes in the electricity price or the incentives in order to encourage the consumers to reduce power consumption at times when the wholesale market prices are high. In Refs. [3,12], an energy management is introduced that can supply consumers with thermal and electrical loads at minimum cost. To this end, a price-based DRP has been used. In Ref. [13], an incentive-based DRP has been proposed in which the load curtailment is considered as a virtual generation unit. In Ref. [14] based on the communication between smart loads and the microgrid agent, information such as load priority is given to the microgrid agent. Based on load information, e.g., priority, power supply to loads is determined by microgrid agent. Based on the priority of loads and in peak hours, low priority loads are curtailed, medium-priority loads are shifted to off-peak hours, and high priority loads are fully supplied. In Ref. [15], demand side announces its load curtailment bidding and microgrid central controller applies the accepted contracts for virtual generation in order to supply loads during peak hours. However, the majority of studies have not considered both price- and incentive-based DRPs in the energy management of microgrids and also their impact on system operation.

There are many approaches to solve the microgrid energy management problem. These methods can be divided into two general categories, namely mathematical and heuristic. There are some mathematical methods that are used in scheduling microgrid resources such as linear programming [16], nonlinear programming [10] and mixed-integer linear programming [17] and [18]. Heuristic methods like Cuckoo Optimization Algorithm [5], Particle Swarm Optimization (PSO) [1], Whale Optimization Method [4], Adaptive Modified Firefly Algorithm (AMFA) [6], Binary coding Gravitational Search Algorithm (BGSA) [7] and θ-PSO [19] have also been used to solve the problem of microgrid energy management.

In the present study, the microgrid energy management is employed while considering various types of DERs and DRPs in order to supply consumers with thermal and electrical loads at minimum cost. As demonstrated in Table 1, the present study in comparison to other studies has used various types of DERs in the microgrid energy management. The aforementioned resources include renewable resources of wind turbine and PV modules, non-renewable resources such as CHP units, fuel cells, heat buffer tank, power only units, heat only unit, and PEVs. For modeling the technical constraints of CHP units, both convex and non-convex FORs have been considered. The majority of studies have not considered both price- and incentive-based DRPs in the energy management of microgrid, but in this study, both price- and incentive-based DRPs along with modeling the cost of load readiness have been used with the purpose of consumption management. A two-stage stochastic objective function has been used to minimize the operational cost of microgrid. Furthermore, the

uncertainty of market price, electrical load, wind speed and solar radiation is taken into account in order to obtain more realistic results. By using the PDF of uncertain parameters and dividing them, a set of scenarios has been generated. Then, a scenario-reduction method based on optimization is exploited to reduce the number of scenarios. Fig. 1 illustrates the structure of the microgrid discussed in this paper.

The contributions of this paper are summarized as follows:

- The energy management of a microgrid, which includes electrical and thermal loads, with the aim of reducing the operational cost.
- The application of DERs of wind turbine, PV modules, CHP systems, fuel cells, power only units, heat only unit, heat buffer tank, and PEVs in the microgrid energy management. Besides, implementing both price-based and incentive-based DRPs.
- The uncertainty of market price, electrical load, wind speed and solar radiation are taken into account, and scenarios are generated by discretization of PDFs of each uncertain parameter.
- The application of a scenario reduction method based on mixed-integer linear optimization to reduce the number of scenarios.
- Evaluation of the proposed energy management method by investigating and comparing the results of three case studies: grid-connected, grid-connected with DRPs, and island mode with DRPs.

This paper is organized as follows: section 'Mathematical model' gives the mathematical model of DGs, DRPs, PEV, thermal energy storage and objective function. Section 'Scenario generation and reduction' describes the methods of generating scenarios and reducing them. Section 'Case study' investigates three cases of grid-connected, grid-connected with DRPs and island mode with DRPs, to evaluate the effectiveness of the proposed method for microgrid energy management. Finally, section 'Conclusion' gives the conclusion of this paper.

2. Mathematical model

In this section, the mathematical model of objective function along with operational constraints of microgrid and DERs are presented.

2.1. DG

DG includes traditional generation units such as gas micro-turbines and non-traditional generation units like PV modules and wind turbines. Unlike traditional dispatchable units, the generation capacity of renewable units are intermittent and dependent on environmental conditions, so the output power of these units is uncertain. In this study, traditional units of CHP, power only, heat only, and fuel cell as well as renewable energy units of wind turbine and PV modules are utilized.

2.1.1. CHP systems

CHP units are used to generate electrical and thermal power. The electrical and thermal output power of CHP are dependent on each other and form a closed curve called FOR on the CHP's power-heat coordinate system. In this study, both first and second type CHP systems are investigated with convex and non-convex FORs, respectively (Fig. 2) [3].

The operational constraints of CHP units are taken from Ref. [3]. Relations (1) and (2) investigate the conditions in which the placement of CHP's operating point in the FOR region would be possible.

$$P^{chp,min}\left(T^{chp}\right) \times I^{chp} \le P^{chp} \le P^{chp,max}\left(T^{chp}\right) \times I^{chp} \tag{1}$$

$$T^{chp,min}\left(P^{chp}\right) \times I^{chp} \le T_{chp} \le T^{chp,max}\left(P^{chp}\right) \times I^{chp} \tag{2}$$

Relations (1) and (2) can be expanded as the set of relations (3)–(7) for the first type CHP which has a convex FOR. According to Fig. 2 (a), relation (3) illustrates the area below the AB line. Relations (4) and (5) model the upper areas of the BC and CD lines, respectively. Relations (6) and (7) also describe the generation limits of electrical and thermal output power.

$$P_{t,i}^{chp} - P_{i,A}^{chp} - \frac{P_{i,A}^{chp} - P_{i,B}^{chp}}{T_{i,A}^{chp} - T_{i,B}^{chp}} \times \left(T_{t,i}^{chp} - T_{i,A}^{chp}\right) \le 0 \tag{3}$$

$$P_{t,i}^{chp} - P_{i,B}^{chp} - \frac{P_{i,B}^{chp} - P_{i,C}^{chp}}{T_{i,B}^{chp} - T_{i,C}^{chp}} \times \left(T_{t,i}^{chp} - T_{i,B}^{chp}\right) \ge -\left(1 - I_{t,i}^{chp}\right) \times M \tag{4}$$

$$P_{t,i}^{chp} - P_{i,C}^{chp} - \frac{P_{i,C}^{chp} - P_{i,D}^{chp}}{T_{i,C}^{chp} - T_{i,D}^{chp}} \times \left(T_{t,i}^{chp} - T_{i,C}^{chp}\right) \ge -\left(1 - I_{t,i}^{chp}\right) \times M \tag{5}$$

$$0 \le P_{t,i}^{chp} \le P_{i,A}^{chp} \times I_{t,i}^{chp} \tag{6}$$

$$0 \le T_{t,i}^{chp} \le T_{i,B}^{chp} \times I_{t,i}^{chp} \tag{7}$$

The generation limit of electrical and thermal power in the second type of CHP is demonstrated in Relations (8)–(16). The second type of CHP possess a non-convex FOR, so it must be split into two separate regions and also write distinct relations for each of them, as shown in Fig. 2 (b). As a result, two binary variables $X_{1,t}$ and $X_{2,t}$ are used that specify the position of CHP's operating point. Therefore, the operating point can be placed in either of the two areas depending on whether the CHP is on or off and this condition is expressed in relation (14). Other relations follow the same trait as in first-type CHP relations.

$$P_{t,i}^{chp} - P_{i,B}^{chp} - \frac{P_{i,B}^{chp} - P_{i,C}^{chp}}{T_{i,B}^{chp} - T_{i,C}^{chp}} \times \left(T_{t,i}^{chp} - T_{i,B}^{chp}\right) \le 0 \tag{8}$$

$$P_{t,i}^{chp} - P_{i,C}^{chp} - \frac{P_{i,C}^{chp} - P_{i,D}^{chp}}{T_{i,C}^{chp} - T_{i,D}^{chp}} \times \left(T_{t,i}^{chp} - T_{i,C}^{chp}\right) \ge 0 \tag{9}$$

$$P_{t,i}^{chp} - P_{i,E}^{chp} - \frac{P_{i,E}^{chp} - P_{i,F}^{chp}}{T_{i,E}^{chp} - T_{i,F}^{chp}} \times \left(T_{t,i}^{chp} - T_{i,E}^{chp}\right) \ge -(1 - X_{1,t}) \times M \tag{10}$$

$$P_{t,i}^{chp} - P_{i,D}^{chp} - \frac{P_{i,D}^{chp} - P_{i,E}^{chp}}{T_{i,D}^{chp} - T_{i,E}^{chp}} \times \left(T_{t,i}^{chp} - T_{i,D}^{chp}\right) \ge -(1 - X_{2,t}) \times M \tag{11}$$

Table 1
Literatures related to microgrid energy management.

Ref. No.	Formulation type		Uncertainty			Solving method		Load		Demand response		DER						CHP		
	Stochastic	Deterministic	Load	Price	WS	SR	Mathematical	Heuristic	Electrical	Thermal	PB	IB	WT	PV	FC	HO	PO	EES	TES	EV	L	NL	FOR
[2]	↘	–	–	↘	↘	↘	–	↘	↘	↘	–	–	↘	↘	↘	↘	–	–	–	–	↘	–	–
[12]	–	↘	–	–	–	–	↘	–	↘	↘	↘	–	–	–	–	–	↘	↘	↘	–	–	↘	↘
[11]	–	↘	–	–	↘	–	↘	↘	↘	↘	–	–	↘	↘	↘	↘	↘	↘	–	–	–	–	–
[3]	↘	–	↘	↘	–	–	↘	–	↘	–	↘	–	–	–	–	↘	↘	↘	↘	–	↘	↘	↘
[5]	–	↘	–	–	–	–	–	↘	↘	↘	–	–	–	–	↘	↘	↘	–	–	–	–	↘	↘
[4]	–	↘	–	–	–	–	–	↘	↘	↘	–	–	–	–	–	↘	↘	–	–	–	–	↘	↘
[1]	↘	–	–	–	↘	↘	–	↘	–	–	–	↘	↘	↘	↘	–	–	–	–	↘	–	–	–
[17]	↘	–	↘	–	↘	↘	↘	–	–	–	–	↘	↘	↘	–	–	–	–	–	–	–	–	–
[7]	↘	–	–	↘	↘	–	–	↘	–	–	–	–	↘	↘	↘	–	↘	↘	–	–	–	–	–
[6]	↘	–	↘	–	↘	↘	↘	–	–	–	–	–	↘	↘	↘	–	↘	↘	–	–	–	–	–
[15]	↘	–	↘	↘	↘	↘	–	↘	–	–	–	↘	↘	↘	↘	–	↘	↘	–	–	–	–	–
[19]	↘	–	↘	↘	↘	↘	–	↘	–	–	–	–	↘	↘	↘	–	↘	↘	–	–	–	–	–
[16]	–	↘	–	–	–	–	↘	–	↘	↘	–	–	–	–	↘	↘	–	↘	–	–	–	–	–
[14]	–	↘	↘	–	–	–	↘	–	↘	–	↘	–	↘	↘	↘	↘	–	↘	–	–	–	–	–
[18]	–	↘	–	–	–	–	↘	–	↘	–	–	–	–	↘	↘	–	–	↘	–	–	–	–	–
[13]	–	↘	–	–	–	–	↘	–	↘	↘	–	↘	↘	–	–	↘	↘	↘	–	–	↘	–	↘
[10]	–	↘	–	–	–	–	↘	–	↘	↘	–	–	–	↘	↘	↘	↘	↘	–	↘	–	–	–
Current paper	↘	–	↘	↘	↘	↘	↘	–	↘	↘	↘	↘	↘	↘	↘	↘	↘	–	↘	↘	–	↘	↘

WS: Wind Speed, SR: Solar Radiation, PB: Price-Based, IB: Incentive-Based, WT: Wind Turbine, FC: Fuel Cell, HO: Heat Only, PO: Power Only, EES: Electrical Energy Storage, TES: Thermal Energy Storage, EV: Electric Vehicle, L: linear, NL: Non-Linear.

$$0 \le P_{t,i}^{chp} \le P_{i,A}^{chp} \times I_{t,i}^{chp} \tag{12}$$

$$0 \le T_{t,i}^{chp} \le T_{i,B}^{chp} \times I_{t,i}^{chp} \tag{13}$$

$$X_{1,t} + X_{2,t} = I_{t,i}^{chp} \tag{14}$$

$$T_{t,i}^{chp} - T_{i,E}^{chp} \le (1 - X_{1,t}) \times M \tag{15}$$

$$T_{t,i}^{chp} - T_{i,E}^{chp} \ge -(1 - X_{2,t}) \times M \tag{16}$$

The cost of CHP units is linearly modeled as shown in relation (17). The aforesaid relation consists of three components, namely fuel cost, start-up and shutdown costs. Fuel cost of CHP units is obtained from Ref. [20].

$$COST_t^{chp} = \sum_{i=1}^{N^{chp}} \left\{ \left(\lambda^{NG} \times \frac{P_{t,i}^{chp} + T_{t,i}^{chp}}{\eta^{chp}} \right) + \left(C_i^{chp,u} \times SU_{t,i}^{chp} \right) + \left(C_i^{chp,d} \times SD_{t,i}^{chp} \right) \right\} \tag{17}$$

2.1.2. Power only unit

The operation cost and technical constraints modeling of micro turbines, which are considered as power only units in this paper, are described in relations (18)–(26) [21]. Relations (18) and (19) present the power generation range of power only units. In relations (20) and (21), the limitations of ramp-up and down rates are expressed, respectively. For modeling the minimum up and down times of power only units, the auxiliary binary variable $Up_{q,m}$ has been employed as shown in relations (22)–(25).

$$0 \le P_{t,q,\zeta,\theta}^{po} \le P_{q,\zeta}^{MAX} - P_{q,\zeta-1}^{MAX} \quad \forall q,\ t, \theta, \zeta = 2, \ldots., N^b \tag{18}$$

$$0 \le P_{t,q,1,\theta}^{po} \le P_{q,1}^{MAX} \quad \forall\ t, q, \theta \tag{19}$$

$$\sum_{\zeta=1}^{N^b} P_{t,q,\zeta,\theta}^{po} - \sum_{\zeta=1}^{N^b} P_{t-1,q,\zeta,\theta}^{po} \le R_q^{up} \times U_{t,q,\theta}^{po} \quad \forall\ t, q, \theta \tag{20}$$

$$\sum_{\zeta=1}^{N^b} P_{t-1,q,\zeta,\theta}^{po} - \sum_{\zeta=1}^{N^b} P_{t,q,\zeta,\theta}^{po} \le R_q^{down} \times U_{t-1,q,\theta}^{po} \quad \forall\ t, q, \theta \tag{21}$$

$$U_{t,q,\theta}^{po} - U_{t-1,q,\theta}^{po} \le U_{t+Up_{q,m},q,\theta}^{po} \quad \forall\ t, q, \theta, m \tag{22}$$

$$U_{t-1,q,\theta}^{po} - U_{t,q,\theta}^{po} \le 1 - U_{t+Dn_{q,m},q,\theta}^{po} \quad \forall\ t, q, \theta, m \tag{23}$$

$$Up_{q,m} = \begin{cases} m & m \le MUT_q \\ 0 & m \ge MUT_q \end{cases} \tag{24}$$

$$Dn_{q,m} = \begin{cases} m & m \le MDT_q \\ 0 & m \ge MDT_q \end{cases} \tag{25}$$

The cost function of the power only units is modeled as a piecewise linear approximation which is shown in Fig. 3 and presented in relation (26).

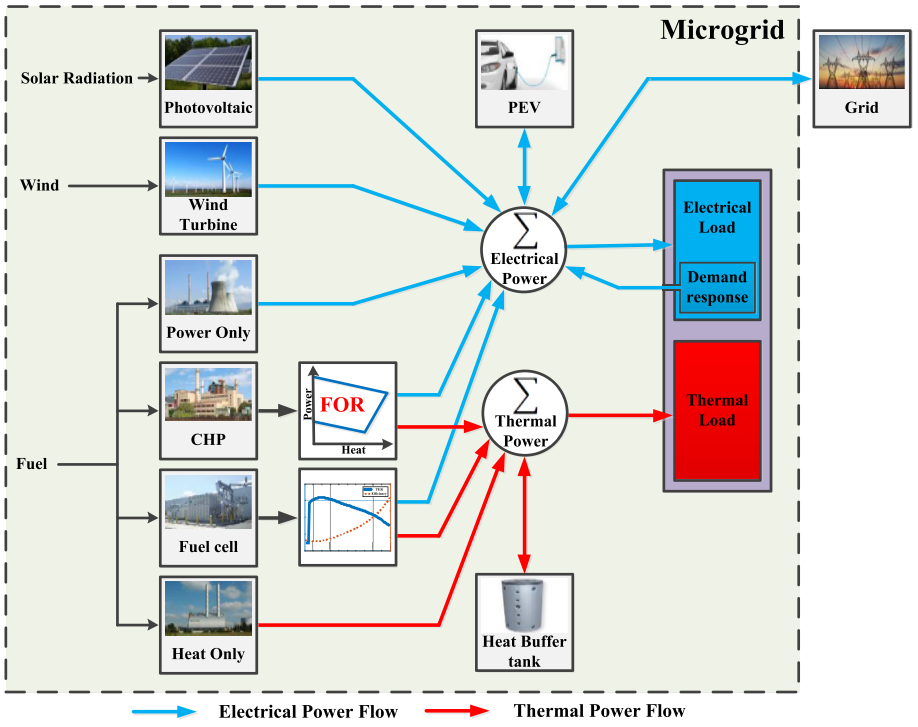

Fig. 1. Structure of microgrid.

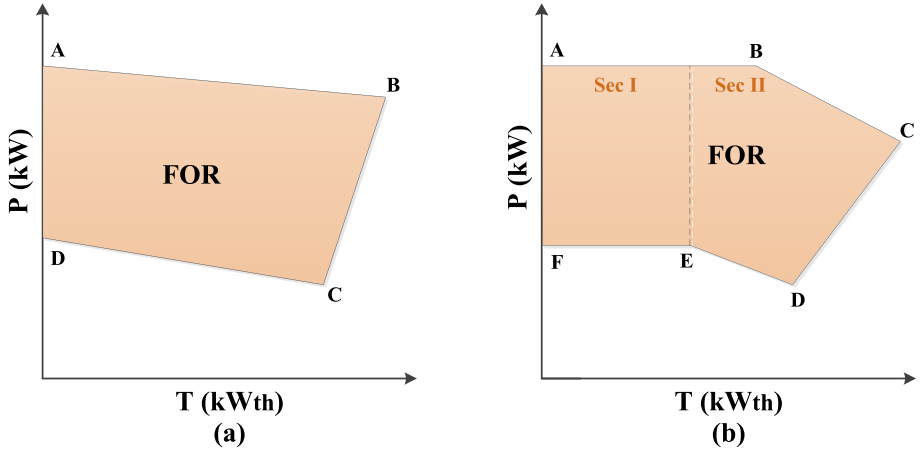

Fig. 2. FOR of CHP units (a) first type, (b) second type.

$$COST^{po}_{t,\theta} = \sum_{q=1}^{N^{po}} \sum_{\zeta=1}^{N^{b}} \lambda^{po}_{q,\zeta} \times P^{po}_{t,q,\zeta,\theta} \quad \forall\, t, \theta \tag{26}$$

2.1.3. Heat only unit

Heat only unit along with fuel cells, CHP units, and heat buffer tank are utilized for supplying thermal loads. The constraint of maximum thermal generation by the heat only unit is presented in relation (27) [3].

$$0 \le T^{ho}_{t} \le T^{ho,max} \quad \forall t \tag{27}$$

Operational cost of heat only unit is expressed in relation (28).

$$COST^{ho}_{t} = \lambda^{ho} \times T^{ho}_{t} \quad \forall t \tag{28}$$

2.1.4. Fuel cell

The thermal and electrical loads of microgrid consumers are partly supplied by Proton Exchange Membrane (PEM) fuel cells (Since these fuel cells can capture and use the by-product heat, they can also be classified as CHP system). During periods of low thermal load, the power between zero and the difference between the maximum capacity and the generated electrical power can be used to produce hydrogen. The hydrogen produced by the fuel cell is stored in a hydrogen tank and converted to the electricity in other time periods to supply electrical load demand in microgrid (of course, in some references, the produced hydrogen can also be

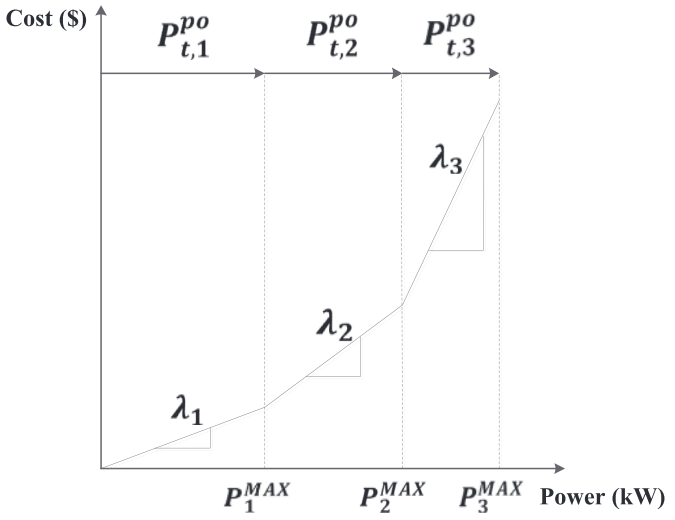

Fig. 3. Piecewise linear approximation of power only unit's cost function.

sold) [22]. Also in the modeling, $P_{t,j}^{fc,h}$ is equivalent electrical power for generated hydrogen. It should be noted that main fuel is hydrogen which is produced by natural gas reforming and hydrogen stored in the hydrogen tank is as a backup fuel [3].

The fuel cell efficiency $\eta_{t,j}^{fc}$ is given by the ratio of the electrical output power to the equivalent input power of fuel, which is shown in relation (29). Fuel cell efficiency is a function of electrical output power to the maximum output power ratio. This ratio is expressed by the $PLR_{t,j}$ variable. The electrical and thermal output power of the fuel cell are dependent on each other. The ratio of thermal to electrical output power is shown by the $TER_{t,j}^{fc}$ variable, which is a function of $PLR_{t,j}$ and is shown in relation (29). Fig. 4 illustrates $TER_{t,j}^{fc}$ and $\eta_{t,j}^{fc}$ as a function of $PLR_{t,j}$. Also, F^{fc} coefficient that is used in relations (33) and (65) is the conversion factor (kg of hydrogen/kW of electric power) used to calculate produced hydrogen and equivalent electric power of discharged hydrogen, in equations (33) and (65), respectively [22,23].

$$\begin{aligned}
&for\ PLR_{t,j} \le 0.05\\
&\eta_{t,j} = 0.272,\ TER_{t,j}^{fc} = 0.68\\
&for\ PLR_{t,j} \ge 0.05\\
&\eta_{t,j} = 0.9033 \times PLR_{t,j}^{5} - 2.996 \times PLR_{t,j}^{4} + 3.6503 \times PLR_{t,j}^{3}\\
&-2.0704 \times PLR_{t,j}^{2} + 0.4623 \times PLR_{t,j} + 0.3747\\
&TER_{t,j}^{fc} = 1.078 \times PLR_{t,j}^{4} - 1.974 \times PLR_{t,j}^{3} + 1.5 \times PLR_{t,j}^{2} - 0.282 \times PLR_{t,j}\\
&+0.6838
\end{aligned} \tag{29}$$

Thermal output power of the fuel cell is calculated by relation (30).

$$T_{t,j}^{fc} = TER_{t,j}^{fc} \times \left(P_{t,j}^{fc,e} + P_{t,j}^{fc,h}\right) \quad \forall t,j \tag{30}$$

Relations (31) and (32) show the electrical output power of fuel cell and hydrogen tank capacity constraints, respectively. The amount of produced hydrogen is presented in relation (33). Relation (34) illustrates the amount of hydrogen stored in tank. The maximum discharge rate of hydrogen tank is shown in relation (35).

$$P_{j,min}^{fc} \times I_{t,j}^{fc} \le P_{t,j}^{fc,e} + P_{t,j}^{fc,h} \le P_{j,max}^{fc} \times I_{t,j}^{fc} \quad \forall t,j \tag{31}$$

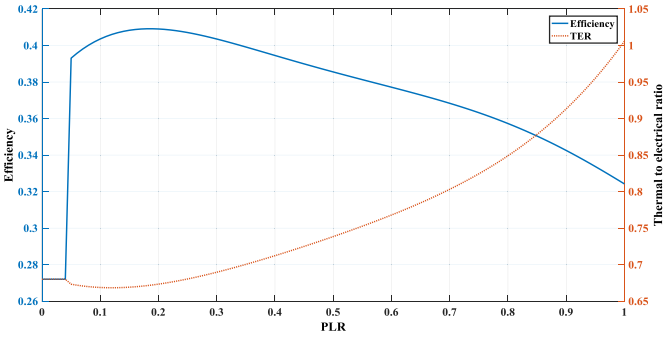

Fig. 4. Operating curve of fuel cell.

$$Cap_j^{fc,h2,min} \le H2_{t,j}^{fc} \le Cap_j^{fc,h2,max} \quad \forall t,j \tag{32}$$

$$H_{t,j}^{fc,h} = F^{fc} \times P_{t,j}^{fc,h} \quad \forall t,j \tag{33}$$

$$H2_{t,j}^{fc} = H2_{t-1,j}^{fc} + \left(\eta_j^{fc,st} \times H_{t,j}^{fc,h}\right) - \left(H_{t,j}^{fc,dch}\right) \quad \forall j, t = 2,\ldots,24 \tag{34}$$

$$0 \le H_{t,j}^{fc,dch} \le H_j^{fc,dch,max} \times I_{t,j}^{fc} \quad \forall j,t \tag{35}$$

Operational cost of fuel cell which is shown in relation (36), includes costs of fuel, hydrogen pumping, startup and shutdown [3].

$$\begin{aligned}
COST_t^{fc} = \sum_{j=1}^{N^{fc}} \Bigg\{ &\left(\lambda^{NG} \times \frac{P_{t,j}^{fc,e} + P_{t,j}^{fc,h}}{\eta_{t,j}^{fc}}\right) + \left(C_j^{fc,pump} \times P_{t,j}^{fc,h} * \eta^{fc,st}\right)\\
&+ \left(C_j^{fc,u} \times SU_{t,j}^{fc} + C_j^{fc,d} \times SD_{t,j}^{fc}\right) \Bigg\} \quad \forall\ t
\end{aligned} \tag{36}$$

2.1.5. Wind turbine

The output power of wind turbine at hour t and scenario θ is a nonlinear function of wind speed which is calculated by relation (37) [21]. In this relation, V_{ci} is the cut-in speed that the turbine blades does not begin to rotate at speeds lower than that and the output power is zero in this condition. At speeds between V_{ci} and V_r, the output power of wind turbine is a third-order nonlinear function of wind speed. At speeds higher than V_r, the output power of wind turbine is maintained at the constant nominal value. At speeds above V_{co}, the wind turbine will mechanically stop and the output power would be zero.

$$P_{t,\theta}^{wind} = \begin{cases} 0 & V_{t,\theta}^{w} \le V_{ci} \\ p_r \times \left(\dfrac{V_{t,\theta}^{w} - V_{ci}}{V_r - V_{co}}\right)^3 & V_{ci} \le V_{t,\theta}^{w} \le V_r \\ p_r & V_r \le V_{t,\theta}^{w} \le V_{co} \\ 0 & V_{t,\theta}^{w} \ge V_{co} \end{cases} \quad \forall\ t,\theta \tag{37}$$

2.1.6. PV module

Relations (38)–(42) are used to calculate the output power of the PV modules. The output power depends on the solar radiation, ambient temperature of the area, and the characteristics of the module itself [24].

$$T_{C_{t,\theta}} = AT_t + sor_{t,\theta} \times \left(\frac{N_{OT} - 20}{0.8}\right) \quad \forall\, t, \theta \tag{38}$$

$$I^{pv}_{t,\theta} = sor_{t,\theta} \times \left[I_{sc} + K_i \times \left(T_{C_{t,\theta}} - 25\right)\right] \quad \forall\, t, \theta \tag{39}$$

$$V^{pv}_{t,\theta} = V_{oc} - K_v \times T_{C_{t,\theta}} \quad \forall\, t, \theta \tag{40}$$

$$P^{pv}_{t,\theta}\left(sor_{t,\theta}\right) = N^{pv} \times FF \times V^{pv}_{t,\theta} \times I^{pv}_{t,\theta} \quad \forall\, t, \theta \tag{41}$$

$$FF = \frac{V_{MPP} \times I_{MPP}}{V_{oc} \times I_{sc}} \tag{42}$$

2.2. Demand response

In DRPs, consumers change their normal consumption patterns in line with market price or incentive tariffs. Therefore, DRPs can be divided into two broad categories: price- and incentive-based.

In price-based programs, consumers change the amount of their consumption and shift it to another time depending on the electricity price. Since the peak demand and price usually occur over same time intervals, this program makes the consumption curve smoother.

Relations (43) and (44) demonstrate a price-based DRP in which $DR^{up}_{t,\theta}$ and $DR^{down}_{t,\theta}$ indicate the load shifting at hour t and scenario θ. Relation (44) shows the constraint of supplying total load within 24 hours. Relations (45) and (46) show the minimum and maximum amount of load shifting at each hour [25].

$$P^{Demand}_{t,\theta} = P^{load}_{t,\theta} + DR^{up}_{t,\theta} - DR^{down}_{t,\theta} \quad \forall\, t, \theta \tag{43}$$

$$\sum_{t=1}^{T} DR^{up}_{t,\theta} = \sum_{t=1}^{T} DR^{down}_{t,\theta} \quad \forall \theta \tag{44}$$

$$0 \le DR^{up}_{t,\theta} \le P^{load}_{t,\theta} \times B^{up}_t \quad \forall\, t, \theta \tag{45}$$

$$0 \le DR^{down}_{t,\theta} \le P^{load}_{t,\theta} \times B^{down}_t \quad \forall\, t, \theta \tag{46}$$

In the second type of DRP, a contract will be signed by customers that the system reliability is not critical for them. When the microgrid goes to the island mode by disturbances in upstream network, the electrical load of these costumers will be curtailed and in exchange they will receive incentives. The cost of incentive-based DRPs falls into two categories. First, the cost of load readiness which acts like a reserve and can be treated via single- or multi-level contracts. Second, the cost of load curtailment which is paid to the consumer if the load is curtailed.

Relation (47) shows the cost of load readiness which is prepared through a three-level contract. Relations (48)–(50) represent the constraints of each level of the contract.

$$COST^{elr}_{t,\theta} = \beta^{\mathrm{I}} \times P^{elr,\mathrm{I}}_{t,\theta} + \beta^{\mathrm{II}} \times P^{elr,\mathrm{II}}_{t,\theta} + \beta^{\mathrm{III}} \times P^{elr,\mathrm{III}}_{t,\theta} \quad \forall t, \theta \tag{47}$$

$$0 \le P^{elr,\mathrm{I}}_{t,\theta} \le \alpha^{\mathrm{I}} \times P^{Demand}_{t,\theta} \quad \forall t, \theta \tag{48}$$

$$0 \le P^{elr,\mathrm{II}}_{t,\theta} \le \alpha^{\mathrm{II}} \times P^{Demand}_{t,\theta} \quad \forall t, \theta \tag{49}$$

$$0 \le P^{elr,\mathrm{III}}_{t,\theta} \le \alpha^{\mathrm{III}} \times P^{Demand}_{t,\theta} \quad \forall t, \theta \tag{50}$$

Relation (51) shows the cost of load curtailment. It is mentioned in the contract (relation (52)) that the amount of load curtailment should not exceed the agreed amount.

$$COST^{elc}_{t,\theta} = \beta^{elc} \times P^{elc}_{t,\theta} \quad \forall t, \theta \tag{51}$$

$$P^{elc}_{t,\theta} \le P^{elr,\mathrm{I}}_{t,\theta} + P^{elr,\mathrm{II}}_{t,\theta} + P^{elr,\mathrm{III}}_{t,\theta} \quad \forall t, \theta \tag{52}$$

If the condition of relation (52) is not satisfied and the load curtailment exceeds the expected amount, then the cost of energy not supplied (ENS) is paid to the costumer. The aforementioned cost is calculated in relation (53).

$$COST^{ens}_{t,\theta} = P^{ens}_{t,\theta} \times \beta^{ens} \quad \forall t, \theta \tag{53}$$

2.3. PEV

The operation modeling of PEVs is presented in relations (54)–(60) [26]. The initial charge of the PEV is illustrated in relation (54). Relation (55) demonstrates the amount of energy in PEV v based on the charged and discharged power at time t and also the stored energy in the previous interval. The relations (56)–(60) demonstrate the operational constraints of PEVs. Relation (57) shows the amount of power that is used to move PEV v at time t. Here, $\Delta D_{t,v}$ is the amount of movement that every vehicle experiences per hour. As presented in (60), it is assumed that each PEV is either in charging ($Uc_{t,v,\theta} = 1$ *and* $Ud_{t,v,\theta} = 0$)/discharging sate ($Uc_{t,v,\theta} = 0$ *and* $Ud_{t,v,\theta} = 1$) or traveling state ($Uc_{t,v,\theta} + Uc_{t,v,\theta} = 0$).

$$SOC_{t_0,v,\theta} = E^0_v \quad \forall t, \theta, v \tag{54}$$

$$SOC_{t,v,\theta} = SOC_{t-1,v,\theta} + \eta^c_v \times Pcv_{t,v,\theta} - \frac{Pdv_{t,v,\theta}}{\eta^d_v} - Ptr_{t,v} \quad \forall\, \theta, v, t = 2, 3, \ldots, T \tag{55}$$

$$SOC^{Min}_v \le SOC_{t,v,\theta} \le SOC^{Max}_v \quad \forall t,\ \theta, v \tag{56}$$

$$Ptr_{t,v} = \Delta D_{t,v} * \Omega_V \quad \forall t, v \tag{57}$$

$$Pc^{Min}_v \times Uc_{t,v,\theta} \le Pc_{t,v,\theta} \le Pc^{Max}_v \times Uc_{t,v,\theta} \quad \forall t\ ,\ \theta, v \tag{58}$$

$$Pd^{Min}_v \times Ud_{t,v,\theta} \le Pd_{t,v,\theta} \le Pd^{Max}_v \times Ud_{t,v,\theta} \quad \forall t, \theta, v \tag{59}$$

$$Uc_{t,v,\theta} + Ud_{t,v,\theta} \le 1 \quad \forall\ t\ ,\ \theta, v \tag{60}$$

2.4. Thermal energy storage

Physical constraints of heat buffer tank are given in relations (61)–(63) [27]. Relation (61) shows the constraint imposed on the

minimum and maximum thermal energy stored in the tank. Moreover, relations (62) and (63) determine the maximum charging and discharging rates of heat buffer tank, respectively.

$$B_{min} \le B_t \le B_{max} \quad \forall t \tag{61}$$

$$0 \le T_t^{b,c} \le T^{b,c,max} \quad \forall t \tag{62}$$

$$0 \le T_t^{b,d} \le T^{b,d,max} \quad \forall t \tag{63}$$

2.5. Power balance

Generated and consumed power at hour t and scenario θ should be equal. The power balance constraint is given in relation (64) and expanded in relation (65):

$$P_{t,\theta}^{eql} = P_{t,\theta}^{Demand} - \left(P_{t,\theta}^{elc} + P_{t,\theta}^{ens}\right) \quad \forall t, \theta \tag{64}$$

$$\begin{aligned} &P_{t,\theta}^{G} + \sum_{i=1}^{N^{chp}} P_{t,i}^{chp} + \sum_{j=1}^{N^{fc}} \left(P_{t,j}^{fc,e} + \frac{H_{t,j}^{fc,dch}}{F^{fc}}\right) + \sum_{q=1}^{N^{po}} \sum_{\zeta=1}^{N^{b}} P_{t,q,\zeta,\theta}^{po} + P_{t,\theta}^{wind} \\ &+ P_{t,\theta}^{PV} + \sum_{v=1}^{N_v} Pd_{t,v,\theta} - \sum_{v=1}^{N_v} Pc_{t,v,\theta} \\ &= P_{t,\theta}^{eql} \quad \forall t, \theta \end{aligned} \tag{65}$$

In the above-mentioned relation, $P_{t,\theta}^{G}$ is the power which is exchanged with the upstream network and it can be either positive or negative. In other words, with respect to the price and demand in each hour, an amount of power is being sold/bought to/from the upstream network.

Total generated thermal power in microgrid can be formulated as relation (66). Although transmission loss of individual units is negligible, since there are multiple CHP units in microgrid, transmission losses should be taken into account.

$$\overline{T}_t = \sum_{i=1}^{N^{chp}} \left(\eta_i^{Tr}\right) \times T_{t,i}^{chp} + T_t^{ho} + \sum_{j=1}^{N^{fc}} T_{t,j}^{fc} \quad \forall t \tag{66}$$

If the start-up and shutdown losses of CHP units are displayed by β_{loss} and β_{gain}, then the amount of generated Thermal power in the microgrid is formulated as relation (67).

$$T_t = \overline{T}_t - \beta_{loss} \times SU_{t,i}^{chp} + \beta_{gain} \times SD_{t,i}^{chp} \quad \forall t, i \tag{67}$$

Relation (68) shows the amount of thermal energy stored in heat buffer tank (standby efficiency of the thermal energy storage is assumed to be 100%) [27]. The thermal power balance constraint is also given in relation (69).

$$B_t = B_{t-1} + \eta^{b,c} \times T_t^{b,c} - \frac{T_t^{b,d}}{\eta^{b,d}} \quad \forall t \tag{68}$$

$$T_t + T_t^{b,d} - T_t^{b,c} = T_t^{load} \quad \forall t \tag{69}$$

2.6. Objective function

Operational cost can be employed as one of the main objective functions in microgrid operational planning. It is assumed that microgrid operator is also the owner of microgrid. The purpose of microgrid energy management is to determine the amount of power generated by the controlled units in the presence of uncontrolled units in a way that besides complying with the operational constraints, the operational cost is also minimized. It is noteworthy that carbon price is not included in the fuel costs and hence the operation cost. For modeling the cost function, a two-stage stochastic programming has been used as shown in relation (70).

$$\begin{aligned} Min\ COST = &\sum_{t=1}^{24} \left(COST_t^{chp} + COST_t^{fc} + COST_t^{ho}\right) + \sum_{\theta=1}^{N^{\theta}} \rho_{\theta} \\ &\times \sum_{t=1}^{24} \left(COST_{t,\theta}^{po} + COST_{t,\theta}^{elr} + COST_{t,\theta}^{elc} + COST_{t,\theta}^{ens} + P_{t,\theta}^{G} \right. \\ &\left. \times \lambda_{t,\theta}^{em}\right) \end{aligned} \tag{70}$$

Stochastic programming technique is a framework for modeling optimization problems that involve uncertainty. This technique in contrast to deterministic methods usually generates more realistic answers and directly covers the deficiencies of deterministic models.

Two-stage stochastic programming models are one type of stochastic programming models. The most important feature of these models is the classification of decision variables into two groups. First, the decision maker takes some action in the first stage, after which a random event occurs, affecting the outcome of the first-stage decision. Then, a recourse decision will be made in the second stage that compensates for any undesirable effects that might have been experienced as a result of the first-stage decision.

In the proposed method of this study for microgrid energy management, the decision-making variables of the first stage that are present in relation (70) are as follows: the output power of CHP units, fuel cells, and heat only unit. Once the weather conditions, electrical load demand, and market price are determined, the decision-making variables of the second stage, including the amount of generated power by power only units, demand response resources, and buying/selling power from/to the energy market are selected in a way that the total operational cost (objective function) is minimized.

3. Scenario generation and reduction

3.1. The method of scenario generation

The majority of models that are similar to real world issues have some parameters that are uncertain in some extent. Wind speed, solar radiation, market price and load are among the uncertain parameters in the scheduling of microgrids. For considering the uncertainty in the proposed model, the scenario-based approach has been employed. The purpose of this method is to determine the optimal solution of the programming problem that has uncertain parameters at the time of decision, but their probability distribution is known based on historical data. Then, the PDF is divided into several sections and for each uncertain parameter, a finite number of scenarios with a certain probability is obtained. Therefore, all stochastic parameters will depend on a finite set of scenarios. In the next sections, the following steps are going to be taken in order to generate scenarios as described.

3.1.1. Generating PDF for uncertain parameters

In most studies, the Weibull PDF has been used for wind speed

as shown in relation (71) [24]. Here k is the shape index and c the scale index. By the use of mean μ and standard deviation δ values of wind speed, the shape index and scale index will be calculated.

$$PDF(v) = \frac{k}{c}\left(\frac{v}{c}\right)^{k-1} \exp\left(-\left(\frac{v}{c}\right)^{k}\right) \Big| k = \left(\frac{\delta}{\mu}\right)^{-1.086}, c = \frac{\mu}{\Gamma\left(1+\frac{1}{k}\right)} \tag{71}$$

Beta PDF is selected for the solar radiation, which is shown in relation (72) [24]. The variables α and β are beta distribution parameters that are calculated according to relation (72) and with respect to the mean value and standard deviation of the solar radiation.

$$PDF(sor) = \begin{cases} \frac{\Gamma(\alpha+\beta)}{\Gamma(\alpha)\Gamma(\beta)} \times sor^{\alpha-1}(1-sor)^{(\beta-1)} & 0 \le sor \le 1, \alpha \ge 0, \beta \ge 0 \\ 0, otherwise \end{cases}$$
$$\beta = (1-\mu) \times \left(\frac{\mu \times (1+\mu)}{\sigma^2} - 1\right), \alpha = \frac{\mu \times \beta}{1-\mu} \tag{72}$$

For modeling the uncertain parameters of load and market price, the normal PDF is used which is shown in relation (73) [24]. In this function, μ and δ are the mean and the standard deviation values of the uncertain parameters, respectively.

$$PDF(x) = \frac{1}{\sigma\sqrt{2\pi}} exp\left(-\frac{(x-\mu)^2}{2\sigma^2}\right) \tag{73}$$

3.1.2. Scenario generation

Each uncertain parameter can have infinite values and since it is difficult and practically impossible to decide on an optimization problem with infinite inputs, then the PDF of each parameter must be divided into some finite sections. For instance, Fig. 5 shows the discretization of normal distribution function, which is divided into seven sections.

The probability and the corresponding value of each scenario n_x related to the uncertain parameter x are respectively represented by ρ_{x,n_x} and χ_{x,n_x} and are derived from relations (74) and (75).

$$\rho_{x,n_x} = \int_{x_{start,n_x}}^{x_{end,n_x}} PDF(x)dx \quad n_x = 1, \ldots, N_x \tag{74}$$

$$\chi_{x,n_x} = \frac{1}{\rho_{x,n_x}} \times \left(\int_{x_{start,n_x}}^{x_{end,n_x}} x \times PDF(x)dx\right) \quad n_x = 1, \ldots, N_x \tag{75}$$

Now, for each uncertain parameter, a set of scenarios and corresponding probabilities is obtained. Therefore, the total number of scenarios is calculated according to the multiplication principle from relation (76) and each of them forms a scenario vector.

Assuming that the stochastic parameters are independent of each other, the probability of each scenario vector is obtained by multiplying the occurrence probability of its uncertain parameters, as shown is relation (77).

$$N^{\theta} = \prod_{x} N_x \tag{76}$$

$$\rho_{\theta} = \prod_{x} \rho_{x,\theta} \quad \theta = 1, \ldots, N^{\theta} \tag{77}$$

3.2. Scenario reduction

In this study, the PDF of each uncertain parameter is divided into seven areas and for each parameter seven scenarios have been defined. Therefore, the number of obtained scenarios in one hour will be $(7)^4 = 2401$ and calculating this number of scenarios will be really time-consuming. By using the scenario reduction methods, the initial set of scenarios can be reduced to an equivalent set which has the same probable behavior as the initial set.

The method used in reducing the scenarios is a mixed-integer linear optimization and its objective function is the number of new scenarios. By solving this program, the minimum number of scenario vectors that are similar to the initial set will be obtained.

For determining reduced scenario set, a criterion is used which is as follows: the total probability of new scenario vectors that include the scenario χ_{x,n_x} with the probability ρ_{x,n_x} must be equal to the probability value of the scenario χ_{x,n_x} [28].

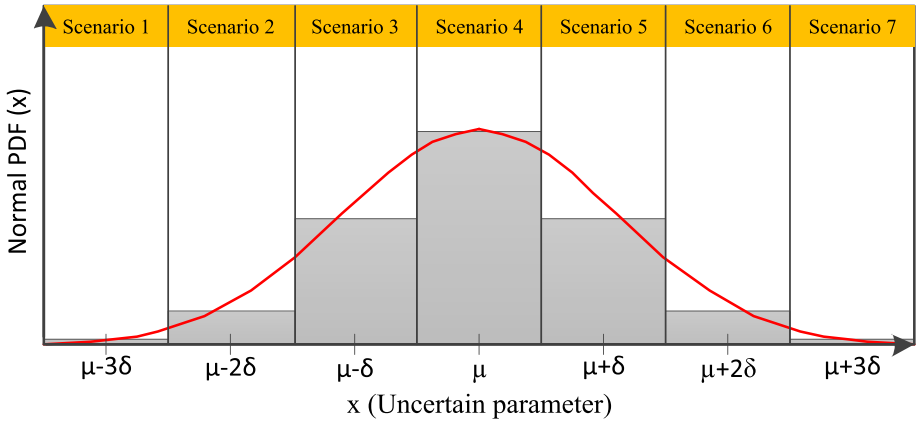

Fig. 5. Discretization of PDF.

$$\min f = \sum_{n_1=1}^{N_1}\sum_{n_2=1}^{N_2}\sum_{n_3=1}^{N_3}\sum_{n_4=1}^{N_4} w_{n_1,n_2,n_3,n_4} \quad (78)$$

s.t

$$\sum_{n_2=1}^{N_2}\sum_{n_3=1}^{N_3}\sum_{n_4=1}^{N_4} \rho_s(n_1,n_2,n_3,n_4) = \rho_{1,n_1} \quad n_1 = 1,2,\ldots,N_1 \quad (79)$$

$$\sum_{n_1=1}^{N_1}\sum_{n_3=1}^{N_3}\sum_{n_4=1}^{N_4} \rho_s(n_1,n_2,n_3,n_4) = \rho_{2,n_2} \quad n_2 = 1,2,\ldots,N_2 \quad (80)$$

$$\sum_{n_1=1}^{N_1}\sum_{n_2=1}^{N_2}\sum_{n_4=1}^{N_4} \rho_s(n_1,n_2,n_3,n_4) = \rho_{3,n_3} \quad n_3 = 1,2,\ldots,N_3 \quad (81)$$

$$\sum_{n_1=1}^{N_1}\sum_{n_2=1}^{N_2}\sum_{n_3=1}^{N_3} \rho_s(n_1,n_2,n_3,n_4) = \rho_{4,n_4} \quad n_4 = 1,2,\ldots,N_4 \quad (82)$$

$$\sum_{n_1=1}^{N_1}\sum_{n_2=1}^{N_2}\sum_{n_3=1}^{N_3}\sum_{n_4=1}^{N_4} \rho_s(n_1,n_2,n_3,n_4) = 1 \quad \forall\ n_1,n_2,n_3,n_4 \quad (83)$$

$$\rho_s(n_1,n_2,n_3,n_4) \le w_{n_1,n_2,n_3,n_4} \quad \forall\ n_1,n_2,n_3,n_4 \quad (84)$$

$$0 \le \rho_s(n_1,n_2,n_3,n_4) \le 1 \quad \forall\ n_1,n_2,n_3,n_4 \quad (85)$$

$$w_{n_1,n_2,n_3,n_4} \in \{0,1\} \quad (86)$$

In the above-mentioned relations, w_{n_1,n_2,n_3,n_4} is a binary variable that specifies whether the scenario vector with variables n_1, n_2, n_3 and n_4 should be selected or not. $\rho_s(n_1,n_2,n_3,n_4)$ is the probability of new scenario vectors. Solving the above-mentioned optimization problem will lead to the minimum number of scenario vectors and their probabilities.

4. Case study

In this paper, three cases are investigated:

Case 1: grid-connected mode without DRPs.
Case 2: grid-connected mode with implementing DRPs, considering maximum possible load shifting up to 10 and 20%.
Case 3: island mode with different types of DRPs, considering maximum possible load shifting up to 10%.

Table 2 shows the average values of the market price, electrical and thermal loads, solar radiation, wind speed and ambient temperature for a 24-hour period. The price of the electricity market is based on the Hourly Ontario Energy Price (HOEP) for August 2016 [29]. Input data for electrical and thermal loads are also adapted from Ref. [30]. The hourly solar radiation is according to the monthly average of data in Ref. [31] for each hour. The data for wind speed and ambient temperature are available in Ref. [32]. The price, load, wind speed, and solar radiation scenarios are shown in Fig. 6. Tables 3–10 show the parameters of DGs, thermal energy storage, PEVs, and DRPs. The travel pattern of PEVs is taken from Ref. [26]. The number of PEVs in Ref. [26] is ten, but in this paper, it is increased from ten to twenty considering the same travel pattern for the next ten PEVs. Also, the required technical input data for the PEVs are provided in Table 3 [26]. The characteristics of the power only units are presented in Table 4 [21]. The data for fuel cells and the hydrogen tanks are given in Table 5 [22]. Table 6 provides operational parameters of CHP units that are taken from Ref. [3] and have been modified according to the problem requirements. Wind turbine and PV modules parameters are shown in Tables 7 and 8 and have been taken from Refs. [21] and [24], respectively. The parameters of heat buffer tank are presented in Table 9 [27]. The parameters of DRPs are provided in Table 10, which are taken from Refs. [24] and [25], and are adjusted in line with electricity market price. The obtained model is solved by mathematical methods and GAMS Toolbox. For solving the MINLP problem, ALPHAECP solver has been employed.

Table 2
Forecasted daily market price, electrical and thermal load, solar radiation, wind speed and ambient temperature.

Hour	Market price ($/MWh)	Electrical load (kW)	Thermal load (kWth)	Solar radiation (kW/m^2)	Wind speed (m/s)	Temperature (°C)
1	55.911	666.36	893.6	0	10.5	24.7
2	49.592	552.96	859.6	0	13.5	24.5
3	50.047	534.6	844.1	0	14.9	24.3
4	43.933	533.52	843.2	0	15.6	24.4
5	47.752	629.64	1002.4	0	19.5	24.5
6	68.417	1000.08	1108.8	0.0052	20.6	26.5
7	111.56	1693.44	1199.4	0.0154	14.4	27.5
8	155.334	1748.52	1219.2	0.1377	14.1	28
9	128.59	1470.96	1119.6	0.2984	11.3	28.5
10	99.887	1331.64	986.4	0.4605	9.7	28.8
11	93.784	1260.36	920.1	0.5913	7	29
12	89.092	1148.04	928.4	0.6446	5.9	29.7
13	87.284	1086.48	900.8	0.6807	8.9	29.8
14	81.725	1050.84	928.4	0.6427	9.5	30
15	79.337	1091.88	878.8	0.6139	10.4	29.8
16	82.987	1246.32	1003.2	0.548	8.8	29.5
17	101.716	1488.24	1022.4	0.4475	7.1	29
18	156.565	1826.28	1112.8	0.2689	8.3	27.7
19	201.701	2216.16	1149.6	0.0829	9.9	26.5
20	202.224	2239.92	1189.2	0	7.5	24.8
21	172.936	2095.2	1092.1	0	8.8	25
22	108.075	1806.84	938.4	0	9.8	24.8
23	74.69	1299.24	930.6	0	9.2	24.6
24	68.505	869.4	904.3	0	8.4	24.8

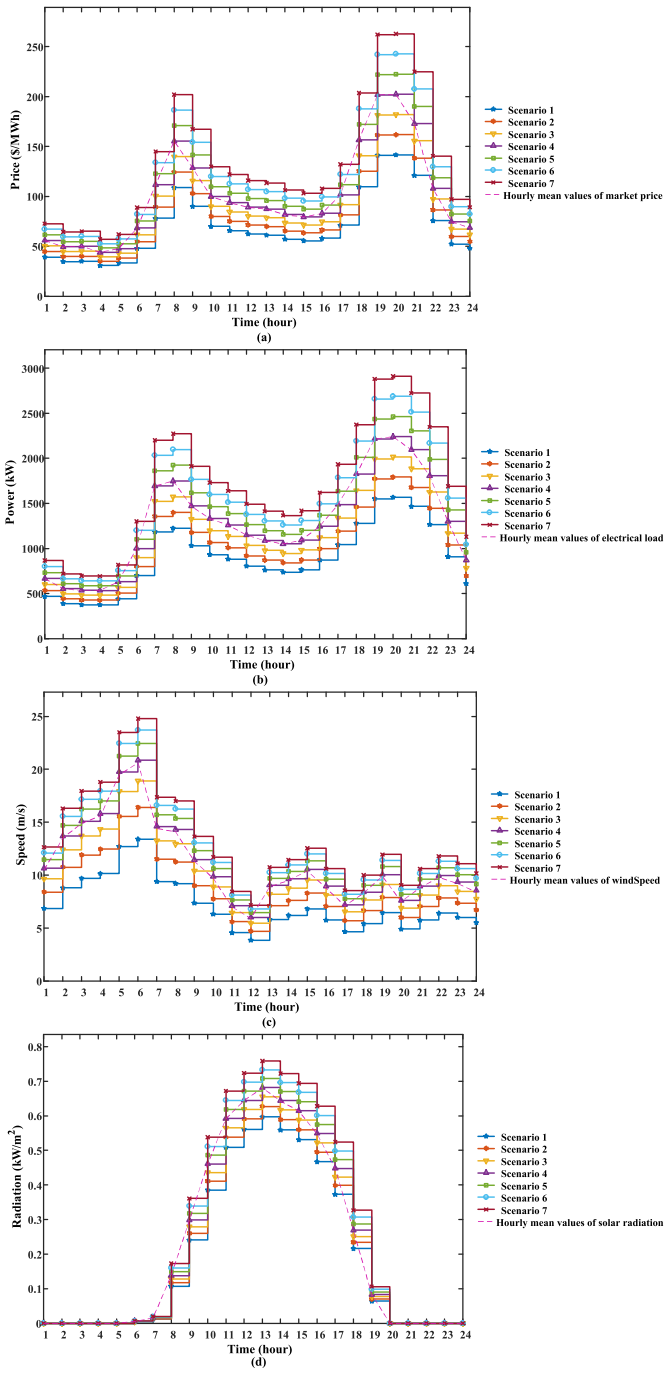

Fig. 6. Scenarios of (a) market price, (b) Electrical load, (c) wind speed and (d) solar radiation.

4.1. Case 1

In this case, it is assumed that the microgrid is connected to grid and exchanges power with the upstream network. The total operational cost is $4143.1562. Fig. 7 shows the power generation of the units, the amount of power exchange with the network, the amount of charging and discharging of PEVs and electrical load demand. Fig. 7 is symmetric and as a result electrical power balance can be obviously observed. Due to the limited capacity of the heat only unit in supplying the thermal load, the operating point of the CHP and fuel cell units will be in a way that the thermal power balance constraint is present. The electrical load is low from 1 to 5 a.m. and the power of wind turbine is high. Therefore, the power only units remain inactive and CHP and fuel cell units are used to supply electrical and thermal loads. PEVs are charged according to their accessibility from 2 to 5 a.m., when the price is in the lowest possible rate. At 3 a.m., since the electrical and thermal output power of the CHP and fuel cell are dependent on each other, the sum of their electrical output power plus wind turbine power in these hours is greater than the amount of electrical load. Even though the market price is not high at this time, the additional power is sold to the market. In the upcoming hours, due to reduced power generation of wind turbines and the increased electricity consumption in contrast to the time-period from 1 to 5 a.m., it is observed that power only units are remained active. CHP and fuel cell units also increase their output power. Due to the increased consumption of electricity and the shortage of generation capacity at 7 and 8 o'clock, power is purchased from the market. It is noteworthy that PEVs are discharged at these hours to reduce the electricity purchased at peak prices. The low price of the market from 2 to 4 p.m. provides the opportunity to buy electricity from the market. The time-periods from 2 to 6 a.m. are similar to 2–6 p.m. in terms of the low market price and it's a suitable time for

Table 3
Parameters of PEVs.

Parameters	Values	Unit	Parameters	Values	Units
SOC_v^{Min}	1	kWh	Pd_v^{Max}	12.5	kW
SOC_v^{Max}	25	kWh	η_v^c	90	%
Pc_v^{Max}	0	kW	η_v^d	93	%
Pc_v^{Max}	12.5	kW	Ω_v	0.1666	kW/km
Pd_v^{Max}	0	kW	N^v	20	–

Table 4
Parameters of power only units.

Parameters	First unit	Second unit	Third unit	Units
Maximum output power	135	160	180	kW
Minimum output power	0	0	0	kW
λ_1^{po}	0.03	0.036	0.039	$/kWh
λ_2^{po}	0.037	0.04	0.045	$/kWh
λ_3^{po}	0.044	0.049	0.054	$/kWh
P_1^{MAX}	50	100	135	kW
P_2^{MAX}	70	110	160	kW
P_3^{MAX}	90	135	180	kW
MUT_q	2	2	2	hour
MDT_q	2	2	2	hour
R_q^{up}	80	90	100	kW/h
R_q^{down}	80	90	100	kW/h

Table 5
Parameters of fuel cell units.

Parameters	First fuel cell	Second fuel cell	Units
P_{min}^{fc}	25	34	kW
P_{max}^{fc}	250	200	kW
$Cap_j^{fc,h2,min}$	0.2	0.2	Kg
$Cap_j^{fc,h2,max}$	14	16	Kg
$C_j^{fc,pump}$	0.012	0.012	$/kW
$H_{t,j}^{fc,dch,max}$	2.3	2.8	Kg/h
$C_j^{fc,u}$	2	2	$
$C_j^{fc,d}$	1	1	$

Table 6
Parameters of CHP units.

Parameters	First CHP					Second CHP						Units
η^{chp}	75					75						%
$C_i^{chp,u}$	2					1.8						$
$C_i^{chp,d}$	1					1						$
η_i^{Tr}	97					97						%
FOR points		A	B	C	D		A	B	C	D	E	F	
	P	263	195	45	56	P	142	142	120	40	48	48	kW
	T	0	210	120	0	T	0	35	118	69	11	0	kWth

Table 7
Parameters of wind turbine.

Parameters	value	Unit
p_r	300	kW
V_{ci}	2	m/s
V_r	14	m/s
V_{co}	25	m/s

Table 8
Parameters of PV modules.

Parameters	value	Unit
N_{OT}	43	(C^O)
I_{MPP}	4.76	(A)
V_{MPP}	17.32	(V)
N^{Pv}	320	–
K_i	0.00122	(A/C^O)
K_v	0.0144	(V/C^O)
I_{sc}	5.32	(A)
V_{oc}	21.98	(V)

Table 9
Parameters of heat buffer tank.

Parameters	value	Unit
B_{min}	0	kWth h
B_{max}	1000	kWth h
$T^{b,c,max}$	20	kWth
$T^{b,c,min}$	20	kWth
$\eta^{b,c}$	95	%
$\eta^{b,d}$	93	%

Table 10
Parameters of DRPs.

	Parameters	value	Unit
Price-based DRP	B_t^{up}	10–20	%
	B_t^{down}	10–20	%
load readiness contract	β^{I}	0.115	$/kWh
	β^{II}	0.125	$/kWh
	β^{III}	0.14	$/kWh
	α^{I}	7	%
	α^{II}	11	%
	α^{III}	15	%
Load curtailment	β^{elc}	2.88	$/kWh
ENS	β^{ens}	4	$/kWh
	α^{ens}	1	%

charging the PEVs. Figs. 8 and 9 show charge, discharge, and SOC of PEVs over a 24-hour period. Regarding the increasing load from 6 to 10 p.m., it is necessary to purchase electricity from the market for supplying the total load. PEVs are also discharged at peak prices. By the reducing of electrical load from 11 to 12 p.m., the power generation of the units will also be reduced. Considering the low price of the market, the electricity will be purchased from the market. In general, the power exchange with network is done for two reasons: to achieve power balance and to reduce the operational cost.

4.2. Case 2

In this case, microgrid is connected to the upstream network and its scheduling is done separately through considering the DRP in two modes with maximum possible load shifting up to 10 and 20%. Fig. 10 shows the new load curve after running the DRPs.

Increasing the maximum percentage of demand that can be shifted from peak periods to off-peak periods makes the load curve smoother. Fig. 11(a) and (b), indicate the generated power of the units, the amount of exchanged power with the network, the amount of charging and discharging power of PEVs and the electrical load demand in the presence of DRP with maximum amount of 10 and 20% load shifting, respectively. By shifting the load from time periods of 7–9 a.m. and 6–10 p.m. (high demand and price periods) to the time periods of 1–6 a.m., 10 a.m. to 6 p.m., and 11–12 p.m. (low demand and price periods), the amount of power purchased from the market will be reduced at peak hours. As a result, the operational cost will also be lower than the results obtained in case 1. Operational cost of microgrid with 10 and 20% load shifting equals $4019.8743 and $3896.6596, respectively. The results show that the implementation of DRP with maximum amount of 10 and 20% load shifting has reduced the total cost as much as $123.2819 and $246.4966, respectively, compared to case 1.

4.3. Case 3

In this case, the microgrid is disconnected from the main grid. In addition to the priced-based DRP with maximum amount of 10% load shifting, the load curtailment with a three-level contract is also employed. When the microgrid is disconnected from the main grid, supplying the total load due to the capacity limitations of the generation units during peak load periods will not be possible; hence the electrical load should be curtailed. Load curtailment increases the operational cost. As an alternative, shifting the loads from peak hours to off-peak hours reduces the load curtailment and also the costs.

As it is shown in Fig. 12, the load is shifted from 7–8 a.m. and 5–10 p.m. to 1–6 a.m., 10 a.m. to 4 p.m., and 11–12 p.m. . Applying the load shifting technique for supplying the entire load in the time-period of 5–10 p.m. is not enough, so it is necessary to use load curtailment. Initially, the first level of contract will be employed which imposes less expenses. Due to the capacity limitations of level one and the increasing load, the second and third levels of the contract will also be used. Also, PEVs are discharged during the periods of high demand and charged at off-peak hours for reducing the operational cost.

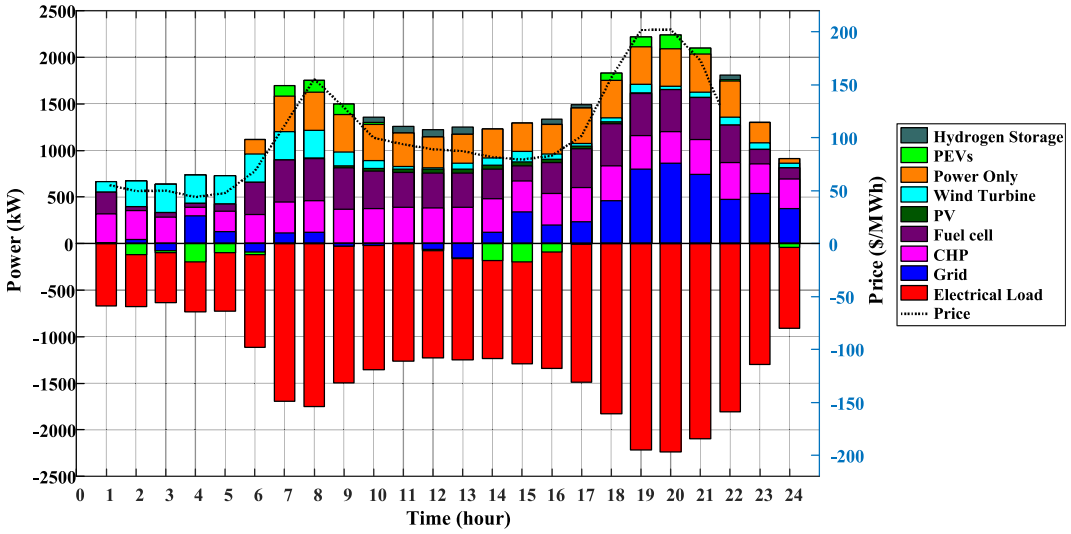

Fig. 7. Generated and consumed electrical power in 24-hour period for case 1.

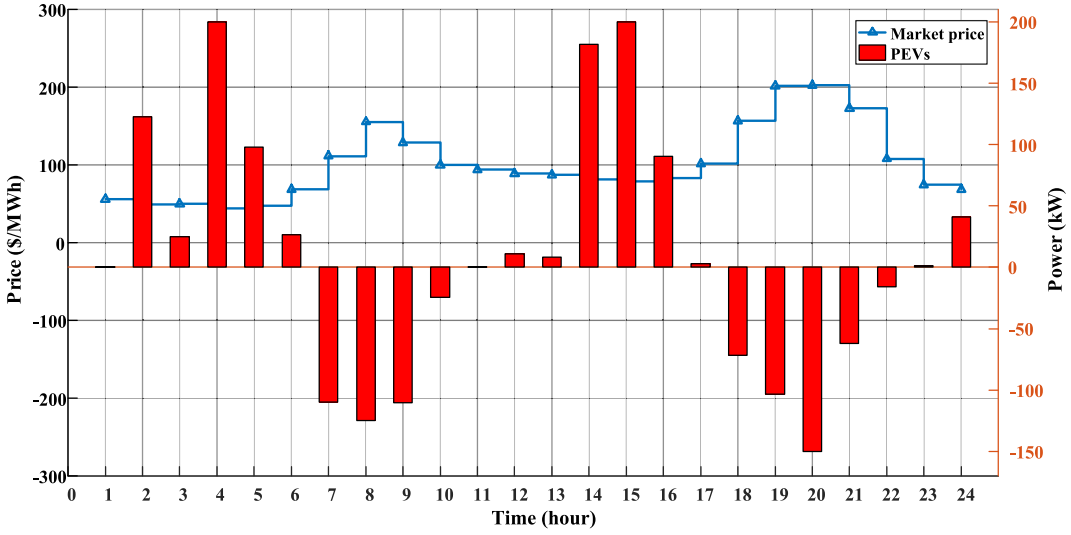

Fig. 8. Charging and discharging power of PEVs for case 1.

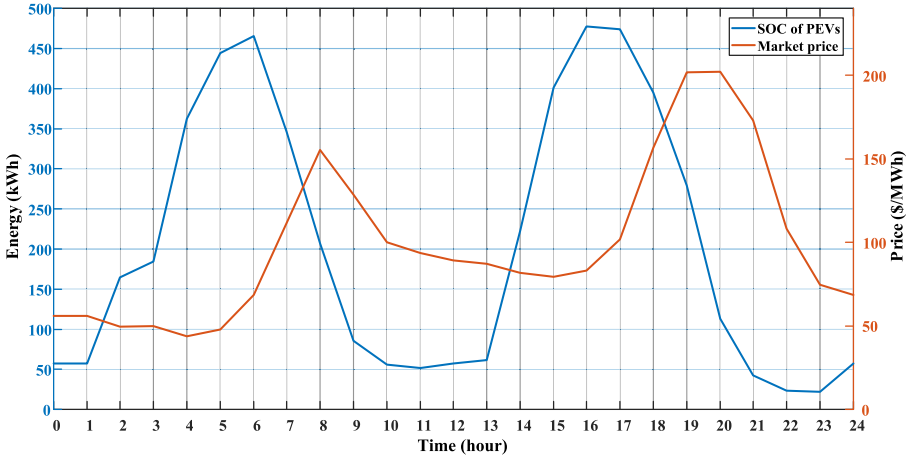

Fig. 9. SOC of PEVs for case 1.

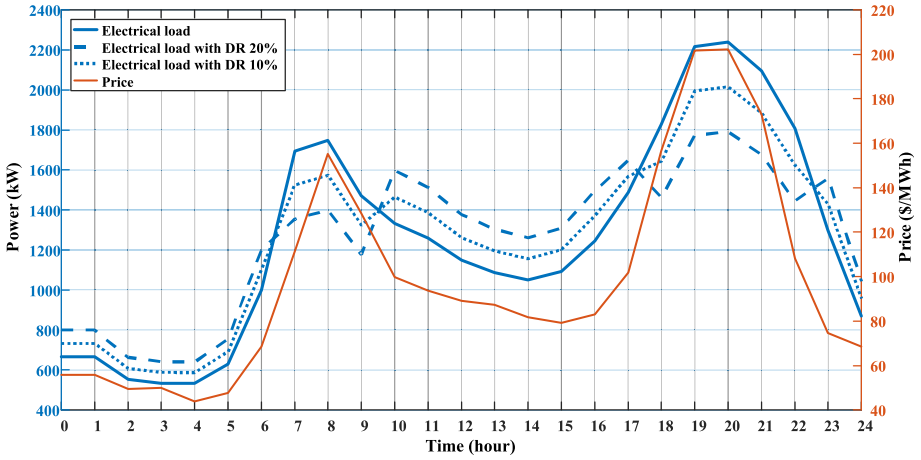

Fig. 10. Electrical load curve before and after implementing price-based DRP.

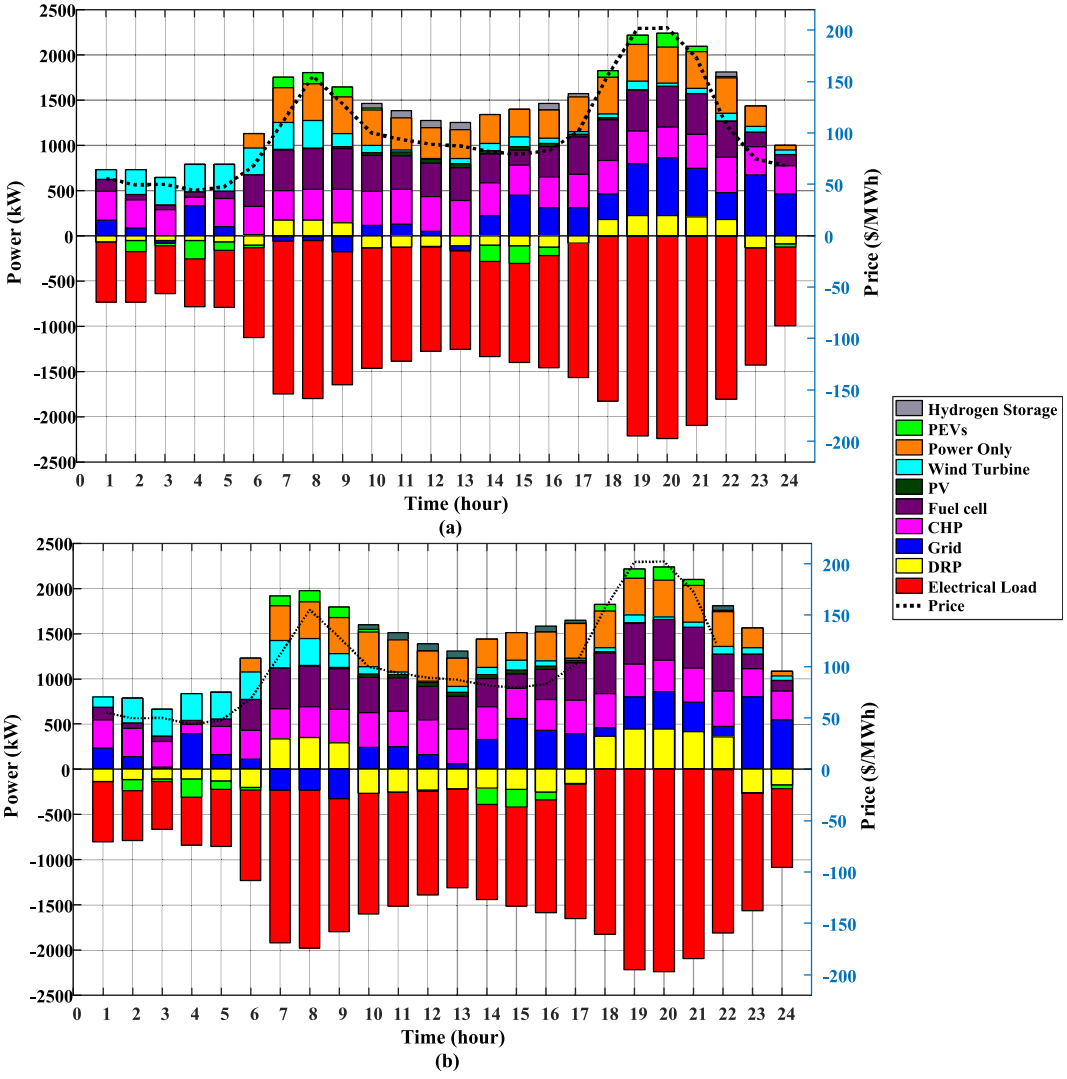

Fig. 11. Generated and consumed electrical power in 24-hour period for case 2 (a) 10% load shifting, (b) 20% load shifting.

The operational cost of case 3 is $12287.7137 which has faced a significant increase in contrast to grid-connected modes and the main reason is the high cost of load curtailment. In general, Table 11 demonstrates the operational cost of the microgrid in aforementioned three cases.

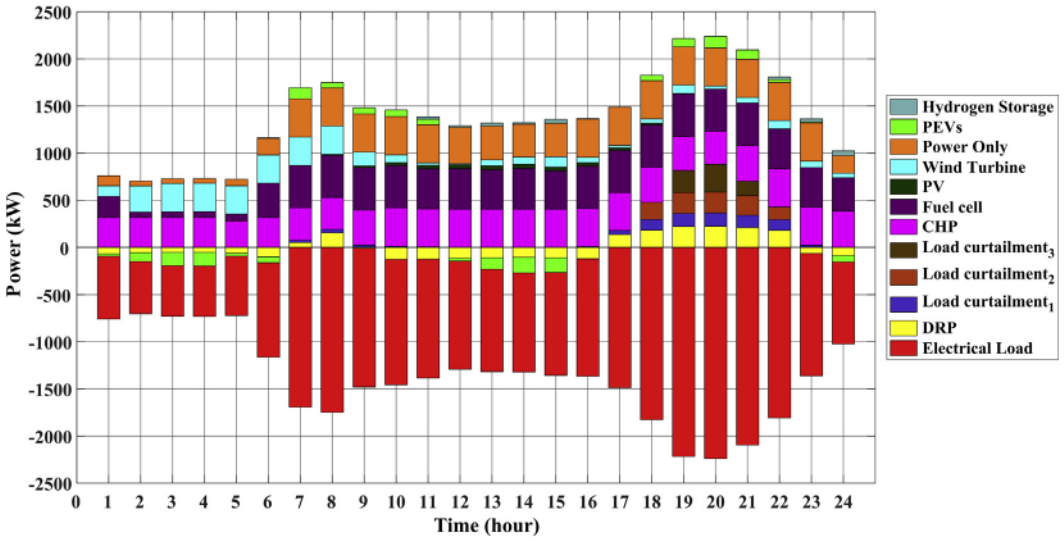

Fig. 12. Generated and consumed electrical power in 24-hour period for case 3.

Table 11
Operational cost of microgrid in different cases.

Case	Connected to grid			Not connected to grid	Unit
	Without DR	DR-10%	DR-20%	DR-10% with load curtailment	
Cost	4143.1562	4019.8743	3896.6596	12287.7137	$

5. Conclusion

A two-stage stochastic programing was used to minimize the operational cost of a microgrid that includes the following resources: wind turbine, PV modules, CHP units, power only units, heat only unit, heat buffer tank and PEVs, to supply electrical and thermal loads. The uncertainty of the market price, load, wind speed and solar radiation are considered in the proposed model. In order to evaluate the proposed model, three cases have been investigated, namely grid-connected without DRPs, grid connected with DRPs, and island mode with DRPs. By comparing the operational cost of the microgrid in grid-connected mode with and without DRP, It is shown that the operational cost reduces by $123.2819 and $246.4966, by implementing 10% and 20% load shifting in case 2, respectively, compared to case 1. Moreover, given that the microgrid does not have the ability to supply the total load in island mode, it is necessary to use incentive-based DRP, and also operational cost increases by $8267.8394 compared to the same grid connected mode. As future work, following contributions will be made:

- Enhancing the proposed method to multi-objective economic/emission operational planning for microgrid energy management.
- Considering the power network model and reducing transmission losses.

References

[1] Rabiee A, Sadeghi M, Aghaeic J, Heidari A. Optimal operation of microgrids through simultaneous scheduling of electrical vehicles and responsive loads considering wind and PV units uncertainties. Renew Sustain Energy Rev 2016;57:721–39.
[2] Bornapour M, Hooshmand R-A, Khodabakhshian A, Parastegari M. Optimal stochastic scheduling of CHP-PEMFC, WT, PV units and hydrogen storage in reconfigurable micro grids considering reliability enhancement. Energy Convers Manag 2017;150:725–41.
[3] Nazari-Heris M, Abapour S, Mohammadi-Ivatloo B. Optimal economic dispatch of FC-CHP based heat and power micro-grids. Appl Therm Eng 2017;114:756–69.
[4] Nazari-Heris M, Mehdinejad M, Mohammadi-Ivatloo B, Babamalek-Gharehpetian G. Combined heat and power economic dispatch problem solution by implementation of whale optimization method. Neural Comput Appl 2017:1–16.
[5] Mehdinejad M, Mohammadi-Ivatloo B, Dadashzadeh-Bonab R. Energy production cost minimization in a combined heat and power generation systems using cuckoo optimization algorithm. Energy Effic 2017;10(1):81–96.
[6] Mohammadi S, Soleymani S, Mozafari B. Scenario-based stochastic operation management of microgrid including wind, photovoltaic, micro-turbine, fuel cell and energy storage devices. Int J Electr Power Energy Syst 2014;54:525–35.
[7] Ji B, Yuan X, Chen Z, Tian H. Improved gravitational search algorithm for unit commitment considering uncertainty of wind power. Energy 2014;67:52–62.
[8] Conejo AJ, Carrión M, Morales JM. Decision making under uncertainty in electricity markets. Springer; 2010.
[9] Li Z, Floudas CA. Optimal scenario reduction framework based on distance of uncertainty distribution and output performance: I. Single reduction via mixed integer linear optimization. Comput Chem Eng 2014;70:50–66.
[10] Derakhshandeh S, Masoum AS, Deilami S, Masoum MA, Golshan MH. Coordination of generation scheduling with PEVs charging in industrial microgrids. IEEE Trans Power Syst 2013;28(3):3451–61.
[11] Sarshar J, Moosapour SS, Joorabian M. Multi-objective energy management of a micro-grid considering uncertainty in wind power forecasting. Energy 2017;139:680–93.
[12] Alipour M, Zare K, Mohammadi-Ivatloo B. Short-term scheduling of combined heat and power generation units in the presence of demand response programs. Energy 2014;71:289–301.
[13] Aghaei J, Alizadeh M-I. Multi-objective self-scheduling of CHP (combined heat and power)-based microgrids considering demand response programs and ESSs (energy storage systems). Energy 2013;55:1044–54.
[14] Zhang L, Gari N, Hmurcik LV. Energy management in a microgrid with distributed energy resources. Energy Convers Manag 2014;78:297–305.
[15] Shi L, Luo Y, Tu G. Bidding strategy of microgrid with consideration of uncertainty for participating in power market. Int J Electr Power Energy Syst 2014;59:1–13.
[16] Moradi M, Khandani A. Evaluation economic and reliability issues for an autonomous independent network of distributed energy resources. Int J Electr Power Energy Syst 2014;56:75–82.
[17] Zakariazadeh A, Jadid S, Siano P. Stochastic multi-objective operational planning of smart distribution systems considering demand response programs. Elec Power Syst Res 2014;111:156–68.

[18] Naraharisetti PK, Karimi I, Anand A, Lee D-Y. A linear diversity constraint–application to scheduling in microgrids. Energy 2011;36(7):4235–43.
[19] Baziar A, Kavousi-Fard A. Considering uncertainty in the optimal energy management of renewable micro-grids including storage devices. Renew Energy 2013;59:158–66.
[20] http://ec.europa.eu/eurostat/documents/38154/42195/Final_CHP_reporting_instructions_reference_year_2016_onwards_30052017.pdf.
[21] Nojavan S, Zare K, Mohammadi-Ivatloo B. Application of fuel cell and electrolyzer as hydrogen energy storage system in energy management of electricity energy retailer in the presence of the renewable energy sources and plug-in electric vehicles. Energy Convers Manag 2017;136:404–17.
[22] El-Sharkh M, Tanrioven M, Rahman A, Alam M. Economics of hydrogen production and utilization strategies for the optimal operation of a grid parallel PEM fuel cell power plant. Int J Hydrogen Energy 2010;35:8804–14.
[23] Dicks Andrew L, Rand David AJ. Fuel cell systems explained. John Wiley Sons; 2018.
[24] Zamani AG, Zakariazadeh A, Jadid S, Kazemi A. Stochastic operational scheduling of distributed energy resources in a large scale virtual power plant. Int J Electr Power Energy Syst 2016;82:608–20.
[25] Wang Y, Ai X, Tan Z, Yan L, Liu S. Interactive dispatch modes and bidding strategy of multiple virtual power plants based on demand response and game theory. IEEE Trans Smart Grid 2016;7(1):510–9.
[26] Soroudi A, Keane A. Risk averse energy hub management considering plug-in electric vehicles using information gap decision theory. In: Plug in electric vehicles in smart grids. Springer; 2015. p. 107–27.
[27] Dolatabadi A, Jadidbonab M, Mohammadi-ivatloo B. Short-term scheduling strategy for wind-based energy hub: a hybrid stochastic/IGDT approach. IEEE Trans Sustain Energy 2018. https://doi.org/10.1109/TSTE.2017.2788086.
[28] Karuppiah R, Martin M, Grossmann IE. A simple heuristic for reducing the number of scenarios in two-stage stochastic programming. Comput Chem Eng 2010;34(8):1246–55.
[29] http://www.ieso.ca/power-data/price-overview/hourly-ontario-energy-price.
[30] Heunis S, Dekenah M. A load profile prediction model for residential consumers in SouthAfrica. In: In domestic use of energy (DUE), 2014 proceedings of the twenty-second. IEEE; 2014 Apr 1. p. 1–6.
[31] http://weather.uwaterloo.ca/data.html.
[32] Nojavan S, Allah Aalami H. Stochastic energy procurement of large electricity consumer considering photovoltaic, wind-turbine, micro-turbines, energy storage system in the presence of demand response program. Energy Convers Manag 2015 Oct 1;103:1008–18.